

[Article]

www.whxb.pku.edu.cn

正十八烷醇在 HOPG 上形成自组装膜的吸附特性

钱丽萍 邓文礼*

(华南理工大学材料科学与工程学院, 广州 510640)

摘要: 研究了正十八烷醇在高定向热解石墨(HOPG)上形成自组装膜的吸附特性, 正十八烷醇在室温下从溶液中吸附至 HOPG 上形成整齐定向排列的单层自组装膜. 通过扫描隧道显微镜(STM)、接触角测量和 X 射线光电子能谱(XPS)分析了正十八烷醇单层自组装膜在 HOPG 上的结构. 实验结果表明, 正十八烷醇自组装膜在基底上成平铺或直立形态, 由于分子在基底上覆盖程度的不同, 会导致它在基底上排列的方式有所不同.

关键词: 高定向热解石墨; 单分子自组装膜; 扫描隧道显微镜; 接触角; X 射线光电子能谱
中图分类号: O647

Adsorption Characteristics of Self-assembled 1-Octadecanol Layer on HOPG

QIAN Li-Ping DENG Wen-Li*

(College of Materials Science and Engineering, South China University of Technology, Guangzhou 510640, P. R. China)

Abstract: Long-chain alkanol, 1-C₁₈H₃₇OH, adsorbed from solution onto highly oriented pyrolytic graphite (HOPG) and formed ordered, oriented monolayer films at room temperature in air. The formation and structure of 1-octadecanol self-assembled monolayers (SAMs) on HOPG were examined using scanning tunneling microscopy (STM), contact angle measurement, and X-ray photoelectron spectroscopy (XPS). Our experimental results indicated that 1-octadecanol SAMs grew in domains, with molecules arranged either horizontally or vertically on the substrate. Moreover, the permutation means of the molecule showed relevance to the surface coverage of 1-octadecanol SAMs on the HOPG.

Key Words: HOPG; SAMs; STM; Contact angle; XPS

The deposition, preparation, and characterization of organic self-assembled surfaces have become an attractive field of fundamental research due to potential applications, e.g. in molecular electronic devices^[1] as well as biosensors^[2-5], biocatalysis, and biotechnology, in general^[6-10]. In this field, there is a very compelling need for methods and procedures yielding high-quality molecular monolayers. Self-chemisorption is particularly an attractive approach to meet the above requirement. It takes advantage of the specific reactivity of molecules and compounds with other molecules and/or the exposed chemical surface groups, giving rise to complex supramolecular architecture. Other methods such as the Langmuir-Blodgett technique or spin coating would hardly be able to provide an assembly of such complex

structures^[11].

Scanning tunneling microscopy (STM) provides a powerful tool for addressing two-dimensional molecular assemblies on a solid surface with atomic or submolecular resolution^[12-15]. As a representative class of physisorbed systems, SAMs of alkanes have been intensively studied on HOPG, MoS₂, and gold surfaces^[16-23]. In comparison with alkanes, alkanol molecules, ending with OH groups at one end, may form additional hydrogen bonds, possibly influencing the structure of their self-assembled monolayers.

In this article, we present a detailed study of the arrangement and binding of 1-octadecanol SAMs on the HOPG, which is attributed to the fact that HOPG is chemically inert and it is easy

Received: October 9, 2007; Revised: December 13, 2007; Published on Web: January 25, 2008.

*Corresponding author. Email: wldeng@scut.edu.cn; Tel: +8620-22236708.

国家自然科学基金(20643001)及广东省科技计划项目(20061311801002)资助

to obtain large-scale atomically flat terraces. The optical and electrical properties of 1-octadecanol deposited on HOPG using the self-assembled layer technique were investigated. The surface morphology, hydrophobic properties, and chemical-bonding characters were monitored by STM, contact angle measurement, and XPS measurement. We propose structural models to explore the bonding mechanism and packing of 1-octadecanol on HOPG surface. Compared with alkanes, hydrogen bonding among the terminal hydroxyl groups in alkanols competes with the adsorbate-substrate and adsorbate-adsorbate interactions among the aliphatic chains, leading to the unique bonding features exhibited by 1-octadecanol on HOPG surface.

1 Experimental

1.1 Preparation of 1-octadecanol SAMs on HOPG

The 1-octadecanol used for the formation of self-assembled monolayer and the tetradecane used as solvent were purchased from ACROS (USA) without further purification. HOPG wafers were purchased from SPI Structure Probe Inc. (West Chester, PA). The concentrations of all the solutions used were less than $0.1 \text{ mmol} \cdot \text{L}^{-1}$. Samples were prepared by depositing a drop of the above solution on freshly cleaved HOPG and by allowing tetradecane to evaporate^[24].

1.2 Contact angle measurement

Contact angles were obtained using the sessile drop method with a JC2000A scientific instrument (Shanghai, China). The drop system calculated the contact angle (θ) from the shape of the drop. Millipore water was used as a probe for contact-angle calculations. For each sample, 3 drops were analyzed on each substrate. The dropped volume was approximately $0.6 \mu\text{L}$, which allowed for ignoring the gravity and considering only the interfacial phenomena. The final contact angle used for calculation or for comparison of different samples was the average of the left and right angles for each drop.

1.3 Scanning tunneling microscopy

The STM measurements were performed with a Digital Instruments Nanoscope IIIA (Santa Barbara, CA) with a Pt/It tips (90/10, 0.25 mm diameter) in air at room temperature. The scanning frequency ranged from 0.1 to 100 Hz. All images were recorded in constant-current mode. A zero-order flattening procedure is used to normalize the vertical offset produced.

1.4 X-ray photoelectron spectroscopy

XPS spectra were recorded using a Kratos Axis Ultra (DLD) (Europe) with a monochromatic Al K_{α} X-ray source (1486.6 eV). The binding energy was calibrated using C 1s (284.6 eV) as an energy standard. The X-ray power and spot size of the analyzer were set at 150 W and $700 \mu\text{m} \times 300 \mu\text{m}$, respectively. The energy resolution of this measurement condition was less than 0.48 eV. The spectra were recorded at a takeoff angle of 80° with pass energy (PE) of 160 eV, a step of 0.1 eV, and a dwell time of 0.1 s for the survey spectra and PE of 40 eV, a step of 0.01 eV, and a dwell time of 1 s for the high-resolution spectra.

2 Results and discussion

2.1 Contact angle

The contact angles for the water on HOPG are close to 100° (99.7° , 98.5° , and 100.9°). The contact angles for the droplet of water on the self-assembled monolayers of 1-octadecanol on HOPG are close to 90° (87.9° , 90.75° , and 89.5°). Fig.1(a) shows the droplet of water on the HOPG surface and Fig.1 (b) shows the droplet of water on the self-assembled monolayers of 1-octadecanol on HOPG. Compared with the 1-octadecanol SAMs, HOPG comprises a densely packed array structure in a horizontal orientation, which leads to a stronger hydrophobic property. So the hydrophobic properties of the HOPG are stronger than those of the 1-octadecanol due to the van der Waals interactions and the monolayer structure. This means the contact angle of 1-octadecanol SAMs is smaller than that of the HOPG. The experimental results are consistent with the theoretical analyses, which reveal that the 1-octadecanol SAMs have been absorbed on HOPG^[25].

2.2 X-ray photoelectron spectroscopy

The data on contact angle support the formation of oriented, self-assembled monolayers at the HOPG surface. Additional confirmation is provided by XPS analysis of the differences between HOPG and the 1-octadecanol SAMs. C 1s and O 1s characteristic peaks appear at the binding energy of 284.68 and 532.68 eV, respectively (Fig.2(a)), which prove that HOPG surface contains oxygen and carbon. Since O 1s content is very low, it is inferred from the XPS analysis that the dissociating oxygen has adsorbed on the HOPG surface. To confirm the chemical state of the carbon element, the analyses mainly focus on C 1s peak, which can be separated into two peaks (284.79 and 285.20 eV) (Fig.2(b)). The binding energy of 284.79 eV is related to the sp^2 conjugated molecule. The binding energy of 285.20 eV is related to the carbon species of the sp^3 conjugated molecule.

Fig.2(c) shows the XPS spectrum of the 1-octadecanol SAMs on HOPG. The content of O 1s characteristic peak (532.61 eV) is 2.234%, which is 0.658% more than that of the pure HOPG whose content of O 1s characteristic peak is 1.576%, which proves that oxygen content increases due to the contribution from —OH. C 1s characteristic peak (284.61 eV) separated into three independent peaks (285.73, 285.19, and 284.79 eV) (Fig.2 (d)). The binding energy of 284.79 eV is contributed by the C atom from the graphite and the —CH₂— species. The binding energy of 285.19 eV is contributed by the C atom from the sp^3

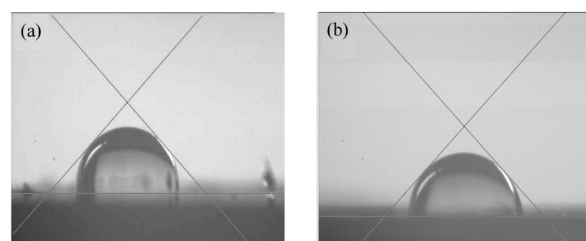


Fig.1 The contact angle for the water on the surface

(a) the droplet of water on the HOPG surface showing a contact angle of approximately 100° ; (b) the droplet of water on the self-assembled monolayers of 1-octadecanol on HOPG showing a contact angle of approximately 90°

conjugated molecule. Compared with the HOPG data, the additional peak at 285.73 eV is contributed by the C atom from the C—O species. The position of a photoelectron peak is sensitive, especially, to the charge density on the unionized atom and to the degree of shielding of the core hole generated by the loss of the electron. For C 1s peaks, this sensitivity manifests itself as chemical shifts to higher binding energies for carbons in higher oxidation states or with electronegative substituents. Through XPS analysis of the surface, we found that 1-octadecanol SAMs have the C—O peak, which the pure HOPG lacks; therefore, it is proved that the 1-octadecanol SAMs self-assemble on the HOPG.

2.3 Scanning tunneling microscopy

A physisorbed monolayer of 1-octadecanol is formed spontaneously after a drop of the solution is deposited on an HOPG surface. Fig.3 shows three packing structures of the 1-octadecanol SAMs on HOPG: the horizontal structure, the staggered structure and the stand-on structure. Fig.3(a) shows the horizontal structure of the 1-octadecanol SAMs on HOPG surface. The alkyl chains of the molecules are parallel to each other. Superimposed lamellar structures are found on the HOPG surfaces and typical reconstruction ridges can be identified. Every lamella is composed of closely packed rods. The length of each rod is consistent with the length of a 1-octadecanol molecule. This finding is in line with previous experimental observations for alkanols on HOPG^[26]. Fig.3(b) shows the staggered structure of the 1-octadecanol SAMs. Fig.3(c) shows the vertical orientation of the end groups of 1-octadecanol SAMs, with the —OH polar groups

facing the HOPG substrates. The bright dots correspond to the methyl groups at the end of hydrocarbon chain. The 1-octadecanol packing is similar to that reported previously^[27].

The images of 1-octadecanol on HOPG have been reported previously^[24,28], and the packing structures of 1-octadecanol SAMs show molecules arranged horizontally on the HOPG surface without the vertically oriented structure of the 1-octadecanol SAMs. However, in our experiment, we found that the 1-octadecanol molecules even could be vertically oriented on their end groups, with the —OH polar groups facing the HOPG substrates at a certain angle. Fig.4 schematically summarizes the proposed self-assembly mechanism. With increasing coverage, the alkanol molecules sequentially adopt a lattice-gas phase, low-density solid phase, and a higher density solid phase. Both solid phases are commensurate, differing mainly in the orientation of the chains. This principal variation we suggested will be adapted to the alkanols with less intermolecular interaction, such as short-chain, methyl-terminated alkanols, and they exhibit a lattice-gas phase that persists under higher lateral pressure before nucleation of solid islands and the solid-solid phase transition occurs by the way of several surface-aligned phases of intermediate density^[29].

In self-assembled structure, long alkyl chain's alkyl-alkyl interaction (two-dimensional crystallization energy) plays a very important role for the fixation of molecules. The alkyl-base interaction plays a decisive role in the permutation orientation of the molecule. So the formation of 1-octadecanol SAMs is determined by van der Waals interactions of alkyl chain with alkyl chain and of alkyl chain with the base^[30,31]. In summary, based on

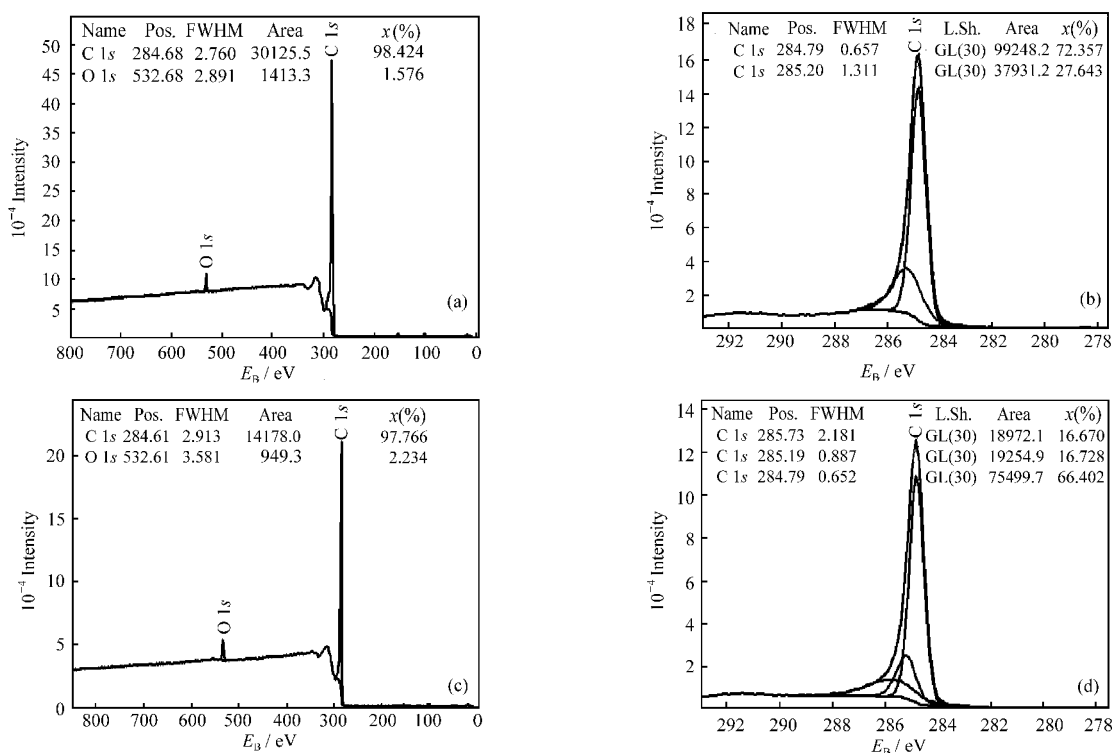


Fig.2 Whole XPS spectrum (a) and typical C 1s XPS spectrum (b) of HOPG; Whole XPS spectrum (c) and typical C 1s XPS spectrum (d) of 1-octadecanol SAMs

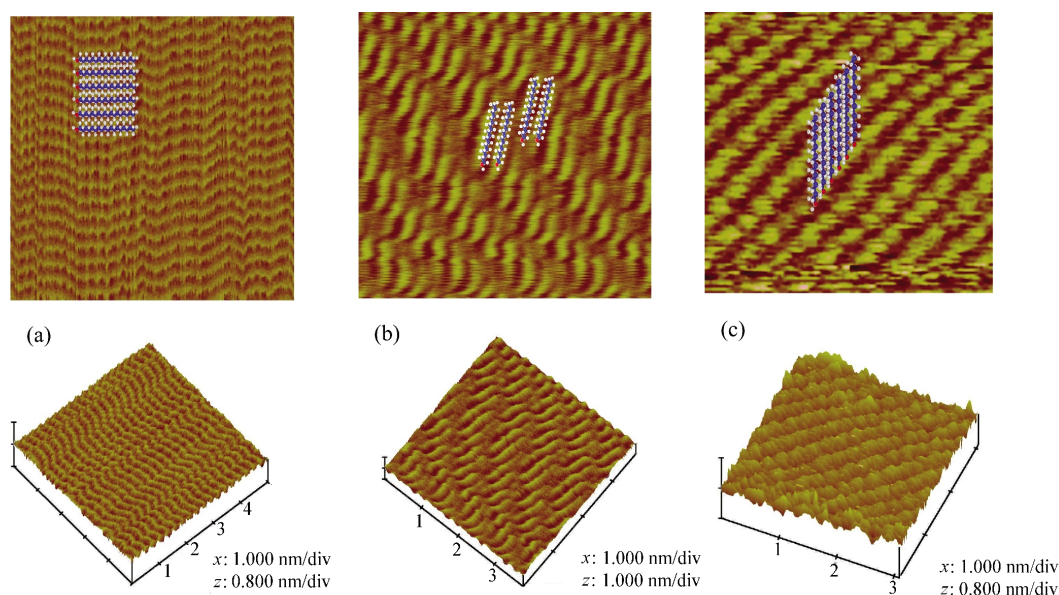


Fig.3 High-resolution STM images of three packing structures of the 1-octadecanol SAMs on HOPG

(a) the horizontal structure of the 1-octadecanol SAMs (10 nm×10 nm, $I=1.12$ nA, $V_b=220$ mV); (b) the staggered structure of the 1-octadecanol SAMs (3.76 nm×3.76 nm, $I=1.20$ nA, $V_b=220$ mV); (c) the vertical orientation of 1-octadecanol SAMs on HOPG (3.07 nm×3.07 nm, $I=1.05$ nA, $V_b=220$ mV)

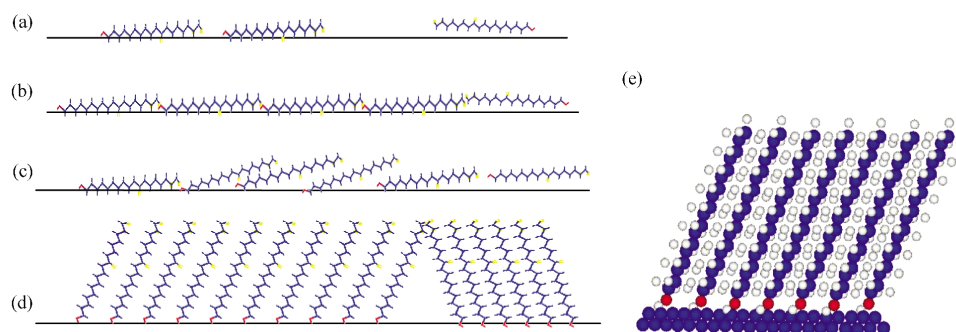


Fig.4 Schematic of self-assembly mechanism for 1-octadecanol on HOPG

(a) alkanols adopt the highly mobile lattice-gas phase at very low coverage; (b) surface reaches saturation coverage; (c) surface undergoes lateral-pressure-induced solid-solid phase transition by nucleation of high-density islands at striped-phase domain boundaries; (d) high-density islands grow at the expense of the striped phase until the surface reaches saturation; (e) the 1-octadecanol SAMs vertically oriented on the HOPG surface

the observations and the schematic, we inferred that the molecules are sequentially arranged on the HOPG surface and form two-dimensional self-assembled monolayer structure. The permutation means of the molecule has relevance to the surface coverage that 1-octadecanol SAMs form on the HOPG.

3 Conclusions

We investigated SAMs of 1-octadecanol molecules on HOPG using contact-angle measurement, XPS, and STM. After comparison of the contact angle of pure HOPG and 1-octadecanol SAMs on HOPG, we inferred that 1-octadecanol formed order-oriented monolayers on HOPG. XPS proved to be a very useful analytical tool for studying both the composition of the monolayer and the elemental profile normal to the surface. The XPS analysis provided further confirmation for 1-octadecanol SAMs adsorbed onto the HOPG surface. Hydroxyl groups in 1-octade-

canol self-assembled monolayers were identified in STM images. 1-octadecanol SAMs grew in domains with molecules either lying horizontally or vertically on the substrate. It was concluded that the 1-octadecanol chains exhibited two permutation means, the parallel type and the staggered type. The permutation means of the molecule had relevance to the surface coverage that 1-octadecanol SAMs form on the HOPG.

References

- Mukhopadhyay, R. *Current Science*, **2003**, *84*(9): 1202
- Weetall, H. H.; Lee, M. J. *Applied Biochemistry and Biotechnology*, **1989**, *22*(3): 311
- Koesslinger, C.; Uttenthaler, E.; Drost, S.; Aberl, F.; Wolf, H.; Brink, G.; Stanglmaier, A.; Sackmann, E. *Sensors and Actuators, B: Chemical*, **1995**, *24*(1-3): 107
- Wang, J.; Jiang, M.; Palecek, E. *Bioelectrochemistry and*

- Bioenergetics*, **1999**, **48**(2): 477
- 5 Kößlinger, C.; Drost, S.; Koch, S. *Biosensors and Bioelectronics*, **1992**, **7**(6): 397
- 6 Gonzalez-Garcia, M. B.; Fernandez-Sanchez, C.; Costa-Garcia, A. *Biosensors and Bioelectronics*, **2000**, **15**(5–6): 315
- 7 Janek, R. P.; Fawcett, W. R.; Ulman, A. *Langmuir*, **1998**, **14**(11): 3011
- 8 Tao, N. J.; Li, C. Z.; He, H. X. *J. Electroanal. Chem.*, **2000**, **49**(2): 81
- 9 Acci, P.; Alliata, D.; Cannistraro, S. *Ultramicroscopy*, **2001**, **89**(4): 291
- 10 Kulin, S.; Kishore, R.; Hubbard, J. B. *Biophysical Journal*, **2002**, **83**(4): 1965
- 11 Tlili, A.; Abdelghani, A.; Aguir, K.; Gillet, M.; Jaffrezic-Renault, N. *Materials Science and Engineering*, **2007**, **27**(4): 620
- 12 Vanoppen, P.; Grim, P. C. M.; Rücker, M. *J. Phys. Chem.*, **1996**, **100**: 19636
- 13 Okawa, Y.; Aono, M. *Nature*, **2001**, **409**: 683
- 14 Grim, P. C. M.; de Feyter, S.; Gesquière, A. *Angew Chem. Int. Ed. Engl.*, **1997**, **36**(23): 2601
- 15 Deng, W. L.; Xiao, Z. W.; Wang, W.; Li, A. D. Q. *J. Phys. Chem. B*, **2007**, **111**: 6544
- 16 Rabe, J.; Buchholz, S. *Science*, **1991**, **253**: 424
- 17 Giancarlo, L. C.; Flynn, G. W. *Annu. Rev. Phys. Chem.*, **1998**, **49**: 297
- 18 Cincotti, S.; Rabe, J. P. *Appl. Phys. Lett.*, **1993**, **62**: 3531
- 19 Ikai, A. *Surf. Sci. Rep.*, **1996**, **26**: 263
- 20 Yamada, R.; Uosaki, K. *J. Phys. Chem. B*, **2000**, **104**: 6021
- 21 He, Y. F.; Ye, T.; Borguet, E. *J. Phys. Chem. B*, **2002**, **106**: 11264
- 22 Xie, Z. X.; Xu, X.; Tang, J.; Mao, B. W. *J. Phys. Chem. B*, **2000**, **104**: 11719
- 23 Zhang, H. M.; Xie, Z. X.; Mao, B. W.; Xu, X. *Chem. Eur. J.*, **2004**, **10**: 1415
- 24 Chen, Y. S.; Zhao, R. G.; Yang, W. S. *Acta. Phys. Sin.*, **2005**, **54**(1): 284 [陈永生, 赵汝光, 杨威生. *物理学报*, **2005**, **54**(1): 284]
- 25 Bain, C. D.; Troughton, E. B.; Tao, Y. T.; Evall, J.; Whitesides, G. M.; Nuzzo, R. G. *J. Am. Chem. Soc.*, **1989**, **111**: 321
- 26 Xie, Z. X.; Xu, X.; Mao, B. W.; Tanaka, K. *Langmuir*, **2002**, **18**: 3113
- 27 Yeo, Y. H.; McGonigal, G. C.; Yackoboski, K.; Guo, C. X.; Thomson, D. J. *J. Phys. Chem.*, **1992**, **96**: 6110
- 28 Buchholz, S.; Rabe, J. P. *Angew Chem., Int. Ed. Engl.*, **1992**, **31**: 189
- 29 Poirier, G. E.; Pylant, E. D. *Science*, **1996**, **272**: 1145
- 30 Yin, S. X.; Wang, C.; Qiu, X. H.; Zeng, Q. D.; Xu, B.; Bai, C. L. *Acta Chim. Sin.*, **2000**, **58**(7): 753 [殷淑霞, 王琛, 裘晓辉, 曾庆涛, 许博, 白春礼. *化学学报*, **2000**, **58**(7): 753]
- 31 Qiu, X. H.; Bai, C. L. *Journal of the Graduate School of the Chinese Academy of Sciences*, **2003**, **20**(1): 107